K. Matsushima, et al., Int. J. Comp. Meth. and Exp. Meas., Vol. 6, No. 6 (2018) 1127–1137

AN INVESTIGATION OF EIGENFREQUENCIES OF BOUNDARY INTEGRAL EQUATIONS AND THE BURTON-MILLER FORMULATION IN TWO-DIMENSIONAL ELASTODYNAMICS

KEI MATSUSHIMA, HIROSHI ISAKARI, TORU TAKAHASHI & TOSHIRO MATSUMOTO
Nagoya University, Japan.

ABSTRACT

In this study, we investigate the distribution of eigenfrequencies of boundary integral equations (BIEs) of two-dimensional elastodynamics. The corresponding eigenvalue problem is classified as a nonlinear eigenvalue problem. We confirm that the Burton-Miller formulation can properly avoid fictitious eigenfrequencies. The boundary element method (BEM) is expected as a powerful numerical tool for designing sophisticated devices related to elastic waves such as acoustic metamaterials. However, the BEM is known that it loses its accuracy for certain frequencies, called as fictitious eigenfrequencies, for problems defined in the infinite domain. Recent researches It has also been revealed that not only the real-valued eigenfrequencies but also the complex-valued ones may affect the accuracy of the BEM results. We examine the distribution of complex eigenvalues obtained by BIEs for time-harmonic elastodynamic problems with the help of the Sakurai-Sugiura method which is applicable to nonlinear eigenvalue problems. We also examine its relation to the accuracy of the BEM numerical results. We also discuss an appropriate choice of the coupling parameter from a viewpoint of the distribution of fictitious eigenfrequencies.

Keywords: Boundary integral equation, Burton-Miller method, Elastodynamics, Fictitious eigenfrequency, Sakurai-Sugiura method, Transmission problem

1 INTRODUCTION

The boundary element method (BEM) is one of the main tools for numerical analyses of various boundary value problems together with the finite element method, finite difference method, and so forth. One of the most remarkable features of the BEM is that it can deal with unbounded domains rigorously without any approximation. This unique property enables us to analyse wave propagation problems, e.g. acoustic, elastic, and electromagnetic waves, defined in the unbounded domain with a high accuracy.

However, the BEM suffers from singularity treatment of the boundary integral equations (BIEs), and also it loses the uniqueness of the solution at certain frequencies, though the original boundary value problem has a unique solution. Those specific frequencies are called fictitious eigenfrequencies, and there existence is a serious drawback of the BEM, especially when the fictitious eigenvalues are real-valued. Thus, some modified BIEs have been proposed to avoid the real-valued fictitious eigenfrequencies, e.g. CHIEF method [1], the Burton-Miller formulation [2], the Müller formulation [3], and the PMCHWT formulation [4].

Recent studies have revealed that not only real-valued eigenfrequencies but also complex-valued ones with small imaginary parts affect the performance of the BEM [5, 6]. This implies that the fictitious eigenfrequency problem may not be avoided even though the modified BIEs are used. In addition, the exterior wave problems and transmission problems also have complex-valued resonance frequencies, which are called true eigenfrequencies in this study. They also affect the boundary element analysis when their imaginary parts are small. We will show later that they are rather small and have bad effects on the analysis in a certain case.

ISSN: 2046-0546 (paper format), ISSN: 2046-0554 (online), http://www.witpress.com/journals
DOI: 10.2495/CMEM-V6-N6-1127-1137

In this study, we investigate the eigenfrequencies of the Burton-Miller-type BIEs in a two-dimensional elastodynamic transmission problem and its relation to the performance of the BEM. The Sakurai-Sugiura method (SSM) [7], which converts a nonlinear eigenvalue problem resulting from the discretized BIEs into a generalised eigenvalue problem, is employed for calculating the eigenfrequencies. Also, we discuss an appropriate choice of the coupling parameter of the Burton-Miller formulation for the elastodynamic problem.

2 BOUNDARY INTEGRAL EQUATIONS

2.1 Problem statement

In this study, we consider a two-dimensional elastodynamic transmission problem. As shown in Fig. 1, let $\Omega^{(1)}$ be an unbounded domain which is filled with a linear isotropic elastic medium whose mass density is $\rho^{(1)}$ and Lamé's constants are $\lambda^{(1)}$ and $\mu^{(1)}$. Similarly, let $\Omega^{(2)} = \mathbb{R}^2 \backslash \Omega^{(1)}$ be a bounded domain with the mass density $\rho^{(2)}$ and their Lamé's constants $\lambda^{(2)}$ and $\mu^{(2)}$. Assuming a plane-strain condition and time harmonic oscillations with time dependence $e^{-i\omega t}$, where ω is the angular frequency. The displacement $\boldsymbol{u}$ and the stress σ in $\Omega^{(1)} \cup \Omega^{(2)}$ are governed by the following transmission problem:

$$\sigma_{ji,j}(x) + \rho^{(1)}\omega^2 u_i(x) = 0 \qquad x \in \Omega^{(1)}, \tag{1}$$

$$\sigma_{ji,j}(x) + \rho^{(2)}\omega^2 u_i(x) = 0 \qquad x \in \Omega^{(2)}, \tag{2}$$

$$u_i^{(1)}(x) = u_i^{(2)}(x)(=: u_i(x)) \qquad x \in \Gamma, \tag{3}$$

$$\sigma_{ji}^{(1)}(x)n_j(x) = \sigma_{ji}^{(2)}(x)n_j(x)(=: t_i(x)) \qquad x \in \Gamma, \tag{4}$$

$$\text{Radiation condition for } u_i^{sc}(x) \text{ as } |x| \to \infty, \tag{5}$$

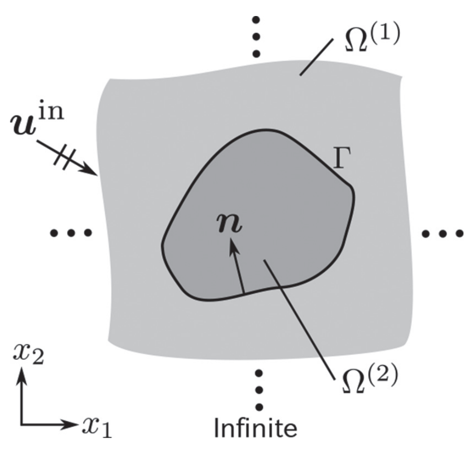

Figure 1: Problem statement.

where $\Gamma = \partial\Omega^{(1)} = \partial\Omega^{(2)}$ is the boundary, $\boldsymbol{n}$ is the unit normal vector on Γ outward to $\Omega^{(1)}$ and $\boldsymbol{u}^{\mathrm{in}}$ and $\boldsymbol{u}^{\mathrm{sc}} = \boldsymbol{u} - \boldsymbol{u}^{\mathrm{in}}$ are the incident and scattered waves, respectively. Also, $\boldsymbol{u}^{(\nu)}$ and $\sigma^{(\nu)}$ ($\nu = 1, 2$) denote the boundary traces of $\boldsymbol{u}$ and σ from $\Omega^{(\nu)}$ to Γ, respectively. The wavenumbers of the longitudinal wave $k_L^{(\nu)}$ and the transverse wave $k_T^{(\nu)}$ in $\Omega^{(\nu)}$ are given by

$$k_{\mathrm{L}}^{(\nu)} = \omega\sqrt{\frac{\rho^{(\nu)}}{\lambda^{(\nu)} + 2\mu^{(\nu)}}}, \tag{6}$$

$$k_T^{(\nu)} = \omega\sqrt{\frac{\rho^{(\nu)}}{\mu^{(\nu)}}}, \tag{7}$$

3 EIGENFREQUENCIES OF THE BIES

3.1 The Burton-Miller-type BIEs in the elastodynamic transmission problem

We obtain the following BIEs equivalent to the transmission problem (1)–(5) by the Burton-Miller formulation:

$$\frac{1}{2}u_i + \frac{\alpha}{2}t_i + \left(D_{ij}^{(1)} + \alpha N_{ij}^{(1)}\right)u_j - \left(S_{ij}^{(1)} + \alpha D_{ij}^{*(1)}\right)t_j = u_i^{\mathrm{in}} + \alpha C_{ijkl}^{(1)} u_{k,l}^{\mathrm{in}} n_j, \tag{8}$$

$$\frac{1}{2}u_i - D_{ij}^{(2)}u_j + S_{ij}^{(2)}t_j = 0, \tag{9}$$

where $\alpha \in \mathbb{C}$ is the coupling parameter, $S_{ij}^{(\nu)}$, $D_{ij}^{(\nu)}$, $D_{ij}^{*(\nu)}$ and $N_{ij}^{(\nu)}$ $(\nu = 1, 2)$ are the integral operators defined for a scalar function w by

$$\left(S_{ij}^{(\nu)}w\right)(x) = \int_\Gamma G_{ij}^{(\nu)}(x, y)\, w(y)\mathrm{d}\Gamma_y, \tag{10}$$

$$\left(D_{ij}^{(\nu)}w\right)(x) = -\mathrm{v.p.}\int_\Gamma C_{kljm}^{(\nu)} G_{ki,l}^{(\nu)}(x, y) n_m(y) w(y)\mathrm{d}\Gamma_y, \tag{11}$$

$$\left(D_{ij}^{*(\nu)}w\right)(x) = \mathrm{v.p.}\int_\Gamma C_{klim}^{(\nu)} G_{kj,l}^{(\nu)}(x, y) n_m(x) w(y)\mathrm{d}\Gamma_y, \tag{12}$$

$$\left(N_{ij}^{(\nu)}w\right)(x) = -\mathrm{p.f.}\int_\Gamma C_{impq}^{(\nu)} C_{kljn}^{(\nu)} G_{kp,lq}^{(\nu)}(x, y) n_m(x) n_n(y) w(\mathrm{y})\mathrm{d}\Gamma_y, \tag{13}$$

where $\boldsymbol{C}^{(\nu)}$ is the elasticity tensor in $\Omega^{(\nu)}$, 'v.p.' and 'p.f.' denote Cauchy's principal value and the finite part of divergent integrals, respectively, and $G_{ij}^{(\nu)}$ is the fundamental solution of two-dimensional elastodynamics which is expressed by the Kronecker delta δ_{ij} and the Hankel function of first kind and order zero $H_0^{(1)}$ as

$$G_{ij}^{(\nu)}(x, y) = \frac{\mathrm{i}}{4\mu^{(\nu)}}\left\{H_0^{(1)}\left(k_T^{(\nu)}|x-y|\right)\delta_{ij} \right.$$
$$\left. + \left(\frac{1}{k_T^{(\nu)}}\right)^2 \frac{\partial^2}{\partial y_i \partial y_j}\left(H_0^{(1)}\left(k_T^{(\nu)}|x-y|\right) - H_0^{(1)}\left(k_L^{(\nu)}|x-y|\right)\right)\right\}. \tag{14}$$

3.2 Classification of the eigenfrequencies of the Burton-Miller-type BIEs

Eigenfrequencies of the Burton-Miller-type BIEs (8) and (9) can be classified into the following three types:

- eigenfrequencies of the boundary value problem (1)–(5) (true eigenfrequencies)
- eigenfrequencies of the interior impedance problem (exterior fictitious eigenfrequencies):

$$C^{(1)}_{ijkl}u_{k,lj}(x)+\rho^{(1)}\omega^2 u_i(x)=0 \qquad x\in\Omega^{(2)}, \tag{15}$$

$$u_i(x)+\alpha C^{(1)}_{ijkl}u_{k,l}(x)n_j(x)=0 \qquad x\in\Gamma. \tag{16}$$

- eigenfrequencies of the exterior Dirichlet problem (interior fictitious eigenfrequencies):

$$C^{(2)}_{ijkl}u_{k,lj}(x)+\rho^{(2)}\omega^2 u_i(x)=0 \qquad x\in\Omega^{(1)}, \tag{17}$$

$$u_i(x)=0 \qquad x\in\Gamma, \tag{18}$$

$$\text{Radiation condition for } u_i(x) \text{ as } |x|\to\infty. \tag{19}$$

3.3 The block Sakurai-Sugiura method (SSM)

The block SSM is a contour integral method which solves a nonlinear eigenvalue problem which finds $\lambda\in\mathbb{C}$ such that there exists a non-trivial solution $\phi\in\mathbb{C}^k$ of

$$A(\lambda)\phi=0, \tag{20}$$

where $A\in\mathbb{C}^{k\times k}$ is an analytic matrix function.

In order to examine eigenfrequencies of the BIEs (8) and (9) numerically, one can set A to be a coefficient matrix which is obtained by discretising the BIEs and perform the block SSM. In this study, however, we limit the shape of the inclusion $\Omega^{(2)}$ to a cylinder of radius a centred at the origin and set A to be

$$\Delta^n_{\text{true}}(\omega)=\begin{bmatrix} U^n_1(a) & U^n_2(a) & -\tilde{U}^n_1(a) & -\tilde{U}^n_2(a) \\ V^n_1(a) & V^n_2(a) & -\tilde{V}^n_1(a) & -\tilde{V}^n_2(a) \\ \mu^{(1)}T^n_{11}(a) & \mu^{(1)}T^n_{12}(a) & -\mu^{(2)}\tilde{T}^n_{11}(a) & -\mu^{(2)}\tilde{T}^n_{12}(a) \\ \mu^{(1)}T^n_{41}(a) & \mu^{(1)}T^n_{42}(a) & -\mu^{(2)}\tilde{T}^n_{41}(a) & -\mu^{(2)}\tilde{T}^n_{42}(a) \end{bmatrix}, \tag{21}$$

$$\Delta^n_{\text{ext}}(\omega)=\begin{bmatrix} \tilde{U}^n_1(a)+\alpha\dfrac{2\mu^{(1)}}{a}\tilde{T}^n_{11}(a) & \tilde{U}^n_2(a)+\alpha\dfrac{2\mu^{(1)}}{a}\tilde{T}^n_{12}(a) \\ \tilde{V}^n_1(a)+\alpha\dfrac{2\mu^{(1)}}{a}\tilde{T}^n_{41}(a) & \tilde{V}^n_2(a)+\alpha\dfrac{2\mu^{(1)}}{a}\tilde{T}^n_{42}(a) \end{bmatrix}, \tag{22}$$

$$\Delta^n_{\text{int}}(\omega)=\begin{bmatrix} U^n_1(a) & U^n_2(a) \\ V^n_1(a) & V^n_2(a) \end{bmatrix}, \tag{23}$$

respectively (see Appendix). This enables us to reduce computational cost and separate the three types of the eigenfrequencies. For general configurations, Misawa *et al.* [6] have proposed a method to distinguish the fictitious eigenfrequencies from the true eigenfrequencies by modifying BIEs.

The nonlinear eigenproblems are solved by the following procedure:

1. Let γ be a closed Jordan curve in the complex plane. Determine a representative point z_0 of γ (e.g. centre of a circle) and compute $A(z_0) = [\boldsymbol{a}_0\ \boldsymbol{a}_1 \cdots\ \boldsymbol{a}_k]$.
2. Construct the Hankel matrices

$$H_{m'} = \begin{bmatrix} \mu_0 & \mu_1 & \cdots & \mu_{m'-1} \\ \mu_1 & \mu_2 & \cdots & \mu_{m'} \\ \vdots & \vdots & \ddots & \vdots \\ \mu_{m'-1} & \mu_{m'} & \cdots & \mu_{2m'-2} \end{bmatrix}, \tag{24}$$

$$H^{<}_{m'} = \begin{bmatrix} \mu_1 & \mu_2 & \cdots & \mu_{m'} \\ \mu_2 & \mu_3 & \cdots & \mu_{m'+1} \\ \vdots & \vdots & \ddots & \vdots \\ \mu_{m'} & \mu_{m'+1} & \cdots & \mu_{2m'-1} \end{bmatrix}, \tag{25}$$

where m' is a sufficiently large integer such that the number of eigenvalues in γ does not exceed m', and the moments μ_i $(i = 0, \cdots, 2m' - 1)$ are defined as

$$\mu_i = \frac{1}{2\pi \mathrm{i}} \int_\gamma z^i f(z) \mathrm{d}z, \tag{26}$$

$$f(z) = U^H \tilde{A}^{-1}(z) V, \tag{27}$$

with the scaled matrix $\tilde{A}(z) = A(z)\ \mathrm{diag}(1/\|a_0\|, 1/\|a_1\|, \ldots, 1/\|a_k\|)$ and random matrices $U, V \in \mathbb{C}^{k\times l}$. If μ_0 is a zero matrix, then we judge that there exists no eigenvalue in γ and terminate the procedure.
3. Compute eigenvalues of , $H^{<}_m - \lambda H_m$ where m is the number of non-zero singular values of $H_{m'}$. The obtained eigenvalues are identical to the eigenvalues of the nonlinear eigenvalue problem $A(\lambda)\phi = \mathbf{0}$ in γ.

4 NUMERICAL EXAMPLES

In this section, we investigate the effect of the eigenfrequencies on the accuracy of the BEM. The collocation method with constant elements is used for discretisation of the BIEs, and GMRES with tolerance 10^{-5} is utilised to solve linear algebraic equations. The boundary Γ is discretised into 500 boundary elements, and its radius is set as $a = 1$ [m]. The incident wave $\boldsymbol{u}^{\mathrm{in}}$ is set to be a plane S-wave propagating in x_2 direction. We first assume the host matrix $\Omega^{(1)}$ to be steel (mass density $\rho = 7.80 \times 10^3$ [kg], Young's modulus $E = 205$ [GPa], Poisson's ratio $\nu = 0.30$) and the inclusion $\Omega^{(2)}$ to be epoxy resin ($\rho = 1.85 \times 10^3$ [kg], $E = 3.00$ [GPa], $\nu = 0.34$).

Figure 2 shows the relative l_2 errors of the numerical solutions $(\boldsymbol{u}, \boldsymbol{t})$ on Γ against the analytical solutions, the numbers of iterations for convergence in the GMRES and the distribution of eigenfrequencies which is obtained by the block SSM. We confirm that the exterior fictitious eigenfrequencies (eigenfrequencies of the interior Dirichlet problem) are distributed only on the real axis but the true and interior fictitious eigenfrequencies are in the lower half-plane. The figure also points out that the accuracy of the BEM and the convergence property

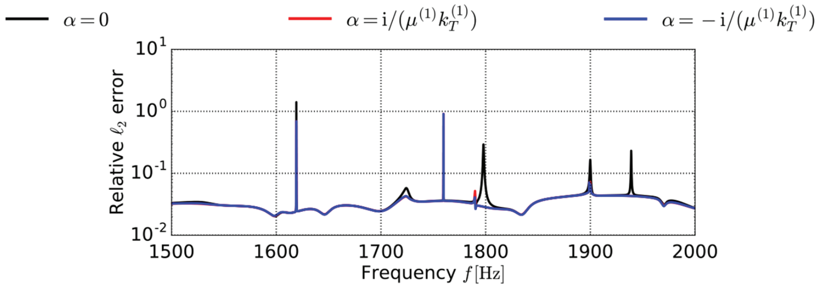

(a) Relative ℓ_2 error against the analytical solution

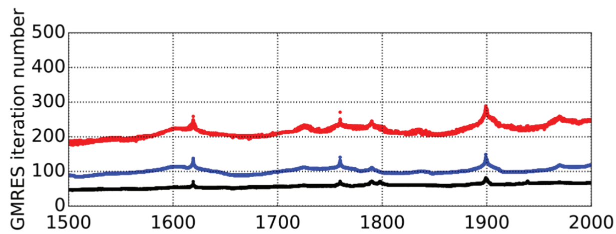

(b) Iteration numbers of the GMRES

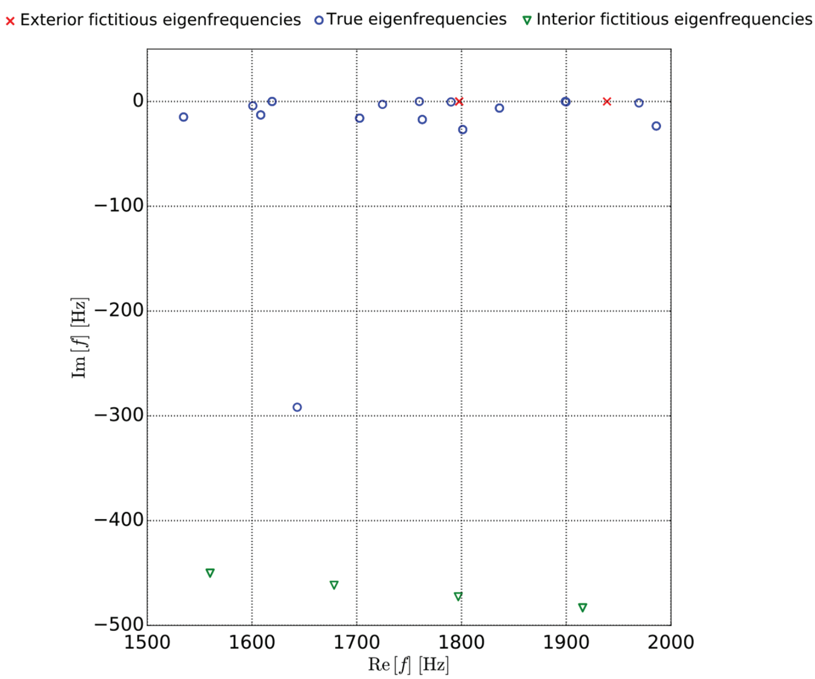

(c) Distribution of the eigenfrequencies in the case of $\alpha = 0$

Figure 2: Relation between the accuracy of the BEM, iteration numbers of the GMRES and distribution of the eigenfrequencies of the BIEs (8), (9) in the case that the host matrix $\Omega^{(1)}$ is the steel and the inclusion $\Omega^{(2)}$ is the epoxy resin.

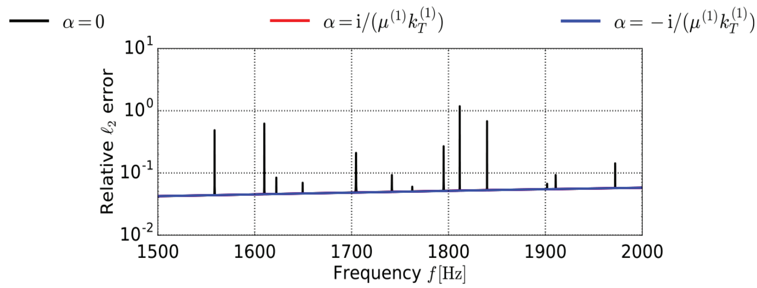

(a) Relative ℓ_2 error against the analytical solution

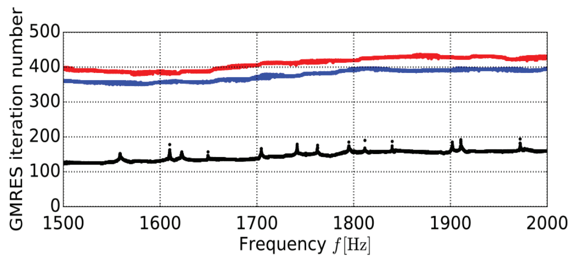

(b) Iteration numbers of the GMRES

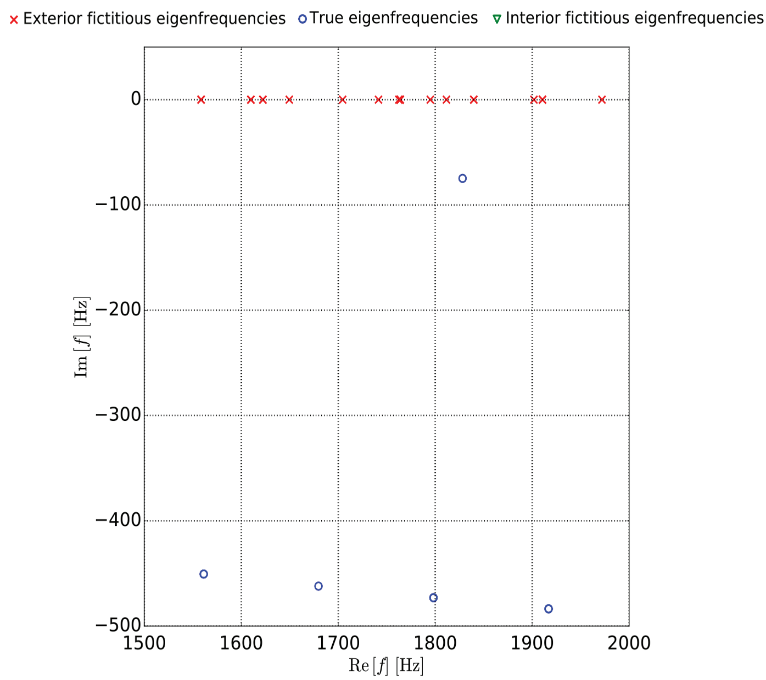

(c) Distribution of the eigenfrequencies

Figure 3: Relation between the accuracy of the BEM, iteration numbers of the GMRES and distribution of the eigenfrequencies of the BIEs (8), (9) in the case that the host matrix $\Omega^{(1)}$ is the epoxy resin and the inclusion $\Omega^{(2)}$ is the steel.

become worse when its frequency is a complex number near the real axis of the complex plane. It is remarkable that not only fictitious eigenfrequencies but also the true eigenfrequencies near the real axis affect the accuracy and convergence property. Note that the effects of the true eigenvalues are inevitable though the fictitious eigenfrequencies can be moved within the complex plane and their effects can be avoided, which will be confirmed below.

Next, we exchange the material parameters of the host matrix and inclusion (the host matrix is the epoxy resin and the inclusion is the steel in this case) and perform the same numerical example. The result is shown in Fig. 3. Different from the previous example, we see that the true eigenfrequencies are not distributed near the real axis and their effects are not observed. In fact, the wavelengths of both the longitudinal and transverse wave in the inclusion $\Omega^{(2)}$ are shorter than in the host matrix $\Omega^{(1)}$ in the previous case, and this would indicate

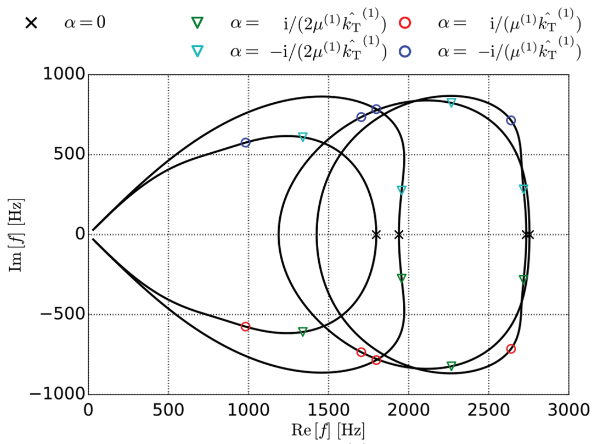

(a) The case that the host matrix $\Omega^{(1)}$ is the steel and the include $\Omega^{(2)}$ is the epoxy resin

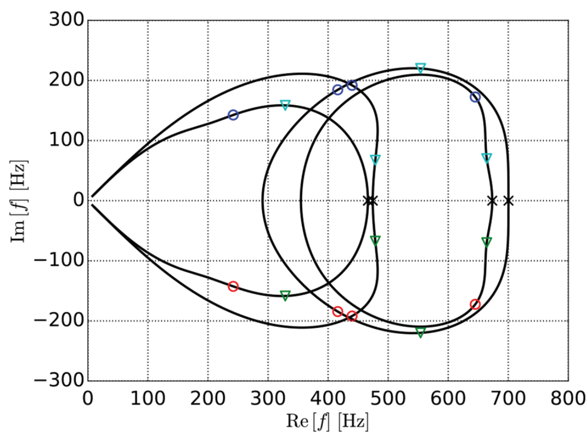

(b) The case that the host matrix $\Omega^{(1)}$ is the epoxy resin and the include $\Omega^{(2)}$ is the steel

Figure 4: Loci of the exterior fictitious eigenfrequencies with variation of $\alpha \in \left\{ \mathrm{i}\,\alpha' / \left(\mu \hat{k}_T^{(1)}\right) \middle|\ \alpha' \in \mathbb{R} \right\}$.

that there exist some eigenmodes with small damping, which is represented as the negative number of the imaginary part of an eigenfrequency (note that the time dependence $e^{-\mathrm{i}\omega t}$ is employed).

Finally, we investigate how the exterior fictitious eigenfrequencies are moved within the complex plane when the coupling parameter α is changed. Considering that some researchers have reported that $\alpha = \pm\mathrm{i}/k$ are appropriate choices for Helmholtz' equations, e.g., [8–10], where k is the wavenumber, we examine α in the form of

$$\alpha = \frac{\mathrm{i}\alpha'}{\mu^{(1)}\hat{k}_T^{(1)}}, \tag{28}$$

where $\alpha' \in \mathbb{R}$ and $\hat{k}_T^{(1)} \in \mathbb{R}$ are parameters which are independent of ω. Practically $\hat{k}_T^{(1)}$ is determined by the target frequency that is actually used in the boundary element analysis. Figure 4 shows loci of some exterior fictitious eigenfrequencies with variation of $\alpha' \in (-\infty, \infty)$. We employ the wavenumber of the transverse wave $\hat{k}_T^{(1)} \in \mathbb{R}$ at the intersection of the locus and real axis as $\hat{k}_T^{(1)}$ for each locus. We see that the loci are symmetric with respect to the real axis for $\alpha' \in (-\infty, 0]$ and $[0, \infty)$, which implies that the distances between the exterior fictitious eigenfrequencies and the real axis are independent of the sign of α' though it significantly affects the convergence property. Also, the loci indicate that $\alpha = \pm\mathrm{i}/\left(\mu^{(1)}\hat{k}_T^{(1)}\right)$ are appropriate choices in the sense of distance from the real axis, and support the results in Figs 2 and 3 that those α can avoid the influence of the exterior fictitious eigenfrequencies. From these results, we conclude that $\alpha = -\mathrm{i}/\left(\mu^{(1)}k_T^{(1)}\right)$ is an appropriate choice of the coupling parameter in the Burton-Miller formulation considering the accuracy and convergence properties.

5 CONCLUSION

In this study, we have investigated a distribution of eigenfrequencies of the Burton-Miller-type BIEs in two-dimensional elastodynamics. The Sakurai-Sugiura method (SSM) has been employed for the investigation. The numerical examples show that the Burton-Miller formulation can avoid the fictitious eigenfrequency problem in terms of the distribution and $\alpha = -\mathrm{i}/\left(\mu^{(1)}k_T^{(1)}\right)$ is an appropriate choice of its coupling parameter.

ACKNOWLEDGEMENTS

This work was supported by JSPS KAKENHI Grant Numbers JP16H04255 and JP17K14146.

APPENDIX: SERIES REPRESENTATION OF WAVE PROPAGATIONS IN TWO-DIMENSIONAL ELASTODYNAMICS

A solution of the equation (1) which satisfies the radiation condition can be written in polar coordinates $x_1 = r\cos\theta$, $x_2 = r\sin\theta$ as follows [11]:

$$u_r(x) = \frac{1}{r}\sum_{n=-\infty}^{\infty}\left(a_n^{(1)}U_1^{n(1)}(r) + b_n^{(1)}U_2^{n(1)}(r)\right)\mathrm{e}^{in\theta} \qquad x \in \Omega^{(1)}, \tag{29}$$

$$u_\theta(x) = \frac{1}{r}\sum_{n=-\infty}^{\infty}\left(a_n^{(1)}V_1^{n(1)}(r) + b_n^{(1)}V_2^{n(1)}(r)\right)\mathrm{e}^{in\theta} \qquad x \in \Omega^{(1)}, \tag{30}$$

$$\sigma_{rr}(x) = \frac{2\mu^{(1)}}{r^2}\sum_{n=-\infty}^{\infty}\left(a_n^{(1)}T_{11}^{n(1)}(r) + b_n^{(1)}T_{12}^{n(1)}(r)\right)\mathrm{e}^{in\theta} \qquad x \in \Omega^{(1)}, \tag{31}$$

$$\sigma_{r\theta}(x)=\frac{2\mu^{(1)}}{r^2}\sum_{n=-\infty}^{\infty}\left(a_n^{(1)}T_{41}^{n(1)}(r)+b_n^{(1)}T_{42}^{n(1)}(r)\right)\mathrm{e}^{\mathrm{i}n\theta} \qquad x\in\Omega^{(1)}, \tag{32}$$

$$\sigma_{\theta\theta}(x)=\frac{2\mu^{(1)}}{r^2}\sum_{n=-\infty}^{\infty}\left(a_n^{(1)}T_{21}^{n(1)}(r)+b_n^{(1)}T_{22}^{n(1)}(r)\right)\mathrm{e}^{\mathrm{i}n\theta} \qquad x\in\Omega^{(1)}, \tag{33}$$

where $a_n^{(\nu)}, b_n^{(\nu)} \in \mathbb{C}$ are constants and $U_i^{n(\nu)}, V_i^{n(\nu)}$ and $T_{ij}^{n(\nu)} (\nu = 1,2)$ are defined as

$$U_1^{n(\nu)}(r)=-nH_n^{(1)}\left(k_L^{(\nu)}r\right)+k_L^{(\nu)}rH_{n-1}^{(1)}\left(k_L^{(\nu)}r\right), \tag{34}$$

$$U_2^{n(\nu)}(r)=\mathrm{i}nH_n^{(1)}\left(k_T^{(\nu)}r\right), \tag{35}$$

$$V_1^{n(\nu)}(r)=\mathrm{i}nH_n^{(1)}\left(k_L^{(\nu)}r\right), \tag{36}$$

$$V_2^{n(\nu)}(r)=nH_n^{(1)}\left(k_T^{(\nu)}r\right)-k_T^{(\nu)}rH_{n-1}^{(1)}\left(k_T^{(\nu)}r\right), \tag{37}$$

$$T_{11}^{n(\nu)}(r)=\left(n^2+n-\frac{1}{2}\left(k_T^{(\nu)}\right)^2r^2\right)H_n^{(1)}\left(k_L^{(\nu)}r\right)-k_L^{(\nu)}rH_{n-1}^{(1)}\left(k_L^{(\nu)}r\right), \tag{38}$$

$$T_{12}^{n(\nu)}(r)=-\mathrm{i}n\left((n+1)H_n^{(1)}\left(k_T^{(\nu)}r\right)-k_T^{(\nu)}rH_{n-1}^{(1)}\left(k_T^{(\nu)}r\right)\right) \tag{39}$$

$$T_{21}^{n(\nu)}(r)=-\left(n^2+n+\frac{\lambda^{(\nu)}}{2\mu^{(\nu)}}\left(k_L^{(\nu)}\right)^2r^2\right)H_n^{(1)}\left(k_L^{(\nu)}r\right)+k_L^{(\nu)}rH_{n-1}^{(1)}\left(k_L^{(\nu)}r\right), \tag{40}$$

$$T_{22}^{n(\nu)}(r)=\mathrm{i}n\left((n+1)H_n^{(1)}\left(k_T^{(\nu)}r\right)-k_T^{(\nu)}rH_{n-1}^{(1)}\left(k_T^{(\nu)}r\right)\right), \tag{41}$$

$$T_{41}^{n(\nu)}(r)=-\mathrm{i}n\left((n+1)H_n^{(1)}\left(k_L^{(\nu)}r\right)-k_L^{(\nu)}rH_{n-1}^{(1)}\left(k_L^{(\nu)}r\right)\right), \tag{42}$$

$$T_{42}^{n(\nu)}(r)=-\left(n^2+n-\frac{1}{2}\left(k_T^{(\nu)}\right)^2r^2\right)H_n^{(1)}\left(k_T^{(\nu)}r\right)+k_T^{(\nu)}rH_{n-1}^{(1)}\left(k_T^{(\nu)}r\right). \tag{43}$$

Similarly, we can obtain a solution of the equation (2) as follows:

$$u_r(x)=\frac{1}{r}\sum_{n=-\infty}^{\infty}\left(a_n^{(2)}\tilde{U}_1^{n(2)}(r)+b_n^{(2)}\tilde{U}_2^{n(2)}(r)\right)\mathrm{e}^{\mathrm{i}n\theta} \qquad x\in\Omega^{(2)}, \tag{44}$$

$$u_\theta(x)=\frac{1}{r}\sum_{n=-\infty}^{\infty}\left(a_n^{(2)}\tilde{V}_1^{n(2)}(r)+b_n^{(2)}\tilde{V}_2^{n(2)}(r)\right)\mathrm{e}^{\mathrm{i}n\theta} \qquad x\in\Omega^{(2)}, \tag{45}$$

$$\sigma_{rr}(x)=\frac{2\mu^{(2)}}{r^2}\sum_{n=-\infty}^{\infty}\left(a_n^{(2)}\tilde{T}_{11}^{n(2)}(r)+b_n^{(2)}\tilde{T}_{12}^{n(2)}(r)\right)\mathrm{e}^{\mathrm{i}n\theta} \qquad x\in\Omega^{(2)}, \tag{46}$$

$$\sigma_{r\theta}(x)=\frac{2\mu^{(2)}}{r^2}\sum_{n=-\infty}^{\infty}\left(a_n^{(2)}\tilde{T}_{41}^{n(2)}(r)+b_n^{(2)}\tilde{T}_{42}^{n(2)}(r)\right)\mathrm{e}^{\mathrm{i}n\theta} \qquad x\in\Omega^{(2)}, \tag{47}$$

$$\sigma_{\theta\theta}(x) = \frac{2\mu^{(2)}}{r^2} \sum_{n=-\infty}^{\infty} \left(a_n^{(2)} \tilde{T}_{21}^{n(2)}(r) + b_n^{(2)} \tilde{T}_{22}^{n(2)}(r) \right) \mathrm{e}^{\mathrm{i}n\theta} \qquad x \in \Omega^{(2)}, \tag{48}$$

where $\tilde{U}_i^{n(v)}, \tilde{V}_i^{n(v)}$ and $\tilde{T}_{ij}^{n(v)}$ are respectively functions which are obtained by replacing the Hankel functions $H_n^{(1)}$ in $U_i^{n(v)}, V_i^{n(v)}$ and $T_{ij}^{n(v)}$ with the Bessel function J_n.

REFERENCES

[1] Schenck, H.A., Improved integral formulation for acoustic radiation problems. *The Journal of the Acoustical Society of America*, **44(1)**, pp. 41–58, 1968. https://doi.org/10.1121/1.1911085

[2] Burton, A.J. & Miller, G.F., The application of integral equation methods to the numerical solution of some exterior boundary-value problems. *Proceedings of the Royal Society of London A: Mathematical, Physical and Engineering Sciences*, **323**, pp. 201–210, 1971. https://doi.org/10.1098/rspa.1971.0097

[3] Müller, C., *Foundations of the Mathematical Theory of Electromagnetic Waves*. Springer Science & Business Media, **155**, 2013.

[4] Chew, W.C., Michielssen, E., Song, J.M. & Jin, J.M., *Fast and efficient algorithms in computational electromagnetics*. Artech House, Inc., 2001.

[5] Misawa, R., Niino, K. & Nishimura, N., An FMM for waveguide problems of 2-D Helmholtz' equation and its application to eigenvalue problems. *Wave Motion*, **63**, pp. 1–17, 2016. https://doi.org/10.1016/j.wavemoti.2015.12.006

[6] Misawa, R., Niino, K. & Nishimura, N., Boundary integral equations for calculating complex eigenvalues of transmission problems. *SIAM Journal on Applied Mathematics*, **77(2)**, pp. 770–788, 2017. https://doi.org/10.1137/16m1087436

[7] Asakura, J., Sakurai, T., Tadano, H., Ikegami, T. & Kimura, K., A numerical method for nonlinear eigenvalue problems using contour integrals. *JSIAM Letters*, **1**, pp. 52–55, 2009. https://doi.org/10.14495/jsiaml.1.52

[8] Kress, R., Minimizing the condition number of boundary integral operators in acoustic and electromagnetic scattering. *The Quarterly Journal of Mechanics and Applied Mathematics*, **38(2)**, pp. 323–341, 1985. https://doi.org/10.1093/qjmam/38.2.323

[9] Amini, S. & Harris, P.J., A comparison between various boundary integral formulations of the exterior acoustic problem. *Computer Methods in Applied Mechanics and Engineering*, **84(1)**, pp. 59–75, 1990. https://doi.org/10.1016/0045-7825(90)90089-5

[10] Zheng, C.J., Chen, H.B., Gao, H.F. & Du, L., Is the Burton-Miller formulation really free of fictitious eigenfrequencies? *Engineering Analysis with Boundary Elements*, **59**, pp. 43–51, 2015. https://doi.org/10.1016/j.enganabound.2015.04.014

[11] Eringen, A.C. & Suhubi, E.S., *Elastodynamics, Vol. II, Linear Theory*. Academic Press, 1975.